The Sequence of Ligand Reductions in Heteroleptic Ruthenium−Diimine Complexes: Calculation of Redox Potentials as a Diagnostic Tool

S. Záliš,* M. Krejčík,† V. Drchal,‡ and A. A. Vlček*,§

J. Heyrovský Institute of Physical Chemistry, Academy of Sciences of the Czech Republic, Dolejškova 3, CZ-18223 Prague 8, Czech Republic

Received October 28, 1994®

The redox potentials of diimine mixed-ligand ruthenium complexes were remeasured under identical conditions. The Hubbard Hamiltonian formalism including solvation contribution was used for the enumeration of the energies of all possible configurations which might come into account in the redox series of these complexes. The comparison of the experimental and calculated half-wave potential sequences based on theoretically calculated electron affinities, combined with analysis of spectra of reduction products, enabled the assignment of electron localization along the redox series.

Introduction

Redox series formed by homoleptic complexes of the type ML_3^{2+} (where L is a diimine type ligand) are well understood. The differences in the redox potential sequence are interpreted in terms of inter- and intraligand electron−electron interactions.[1] The model of the system is based on the assumption of predominantly ligand-based redox changes. Ligand cluster (a supermolecule formed by ligands located in space in the same way as in the real complex) is used as the frame for calculations, the results of which are in reasonable agreement with experiment.[1,2]

The situation is more complex for heteroleptic complexes, $MABC^{2+}$, having several structurally related, albeit not identical ligands (A, B, and C) for which both orbital energies and inter- and intramolecular repulsions differ. It is an accepted practice to assign the various ligand reductions in these complexes according to their orbital energies as reflected in the reduction potentials of the corresponding tris species.

However, some of the results published cast doubt not only upon the assignment of the sequence in which the ligands in a heteroleptic complex are reduced (occupation scheme) but also upon the description of the reduced species as one specific electronic configuration: The reduction pattern of heteroleptic complexes results from a complex interplay of orbital energies and all the various electronic repulsion energies. This could result in the localization of electrons to ligands in a way which can not be deduced from the order of the first reduction potentials of the homoleptic tris species.

To elucidate the problem of electron localization in a heteroleptic complex as it is reduced along a redox series, we extended our previous calculations of homoleptic $ML_3^{(2-n)+}$ complexes to a general complex $MA_mB_{3-m}^{(2-n)+}$ ($m = 0, 1, 2, 3$; $n = 0-6$). Our aim was to obtain a theoretical basis for calculation of the possible sequences of redox potentials in a given redox series. Comparison with the experimental reduction potentials should lead to the most probable occupation pattern along the given redox series.

The main aim of this paper is to devise a simple model which can be used to determine, as a first approximation, the occupation pattern of the heteroleptic complex, supposing the behavior of the corresponding homoleptic species is known. It is shown that the estimated occupation pattern can be, in suitable cases, proved by detailed analysis of spectra of reduction products along the redox series.

Experimental Section

The procedure and equipment used both for electrochemical and spectroelectrochemical measurements have been described previously.[3,4] All redox potentials in this paper are referenced to the first reduction potential of $Ru(bpy)_3^{2+}$ in *N,N'*-dimethylformamide (DMF) containing 0.1 M tetrabutylammonium hexafluorophosphate (TBAH), which is taken as zero (−1.80 V vs Fc^+/Fc couple at −74 °C) .

Complexes were synthesized using either $[Ru(bpy)_2Cl_2]2H_2O$ or $[Ru(bpy)Cl_4]$ as starting materials, prepared according to refs 3 and 4, using a method described in ref 5 or its slight variations. The crude products were purified by column chromatography on activated alumina with acetonitrile or acetonitrile/toluene (1:1) as eluents. The complexes were characterized by their UV−vis absorption spectra. Ligands 2,2'-bipyridine (bpy), 5,5'-bis(ethylcarboxy)-2,2'-bipyridine (5dceb), 4,4'-bis(ethylcarboxy)-2,2'-bipyridine (4dceb), 4,4'-bipyrimidine (bpym), 2,2'-bipyrimidine (bpm), and 2,2'-biquinoline (bq) were either used as obtained commercially or prepared using literature methods (4dceb,[6,7] bpym[8]).

Calculations. The redox potentials of homoleptic tris species were correlated with electron affinities calculated using the procedure applied earlier.[2] It has been assumed that the set of canonical molecular orbitals forming the lowest unoccupied molecular orbitals (LUMO) of the ligand cluster can be transformed into the set of localized orbitals $|1\rangle$, $|2\rangle$, and $|3\rangle$, representing the ligand subsystems A, B, and C, respectively. The electronic structure of the ligand cluster was described by the extended Hubbard (or PPP) Hamiltonian:[9,10]

$$H_H = \sum_{i\sigma} E_i n_{i\sigma} + \sum_i U_i n_{i\uparrow} n_{i\downarrow} + \sum_{i\neq j} V_{ij} n_i n_j \qquad (1)$$

$n_{i\sigma}$ is the occupation operator of the ith state for spin σ, $n_i = n_{i\uparrow} + n_{i\downarrow}$.

† Present address: Colorado State University, Department of Chemistry, Fort Collins, Co 80532.

‡ Present address: Institute of Physics, Na Slovance 2, Prague 8, Czech Republic.

§ Present address: Department of Chemistry, York University, North York (Toronto), Ontario, Canada M3J1P3.

® Abstract published in *Advance ACS Abstracts,* October 15, 1995.

(1) (a) Vlček, A. A. *Coord. Chem. Rev.* **1982**, *43*, 39. (b) Juris, A.; Balzani,V.; Barigelletti, F.; Campana, S.; Belser, P.; von Zelewsky, A. *Coord. Chem. Rev.* **1988**, *84*, 85.
(2) Záliš, S.; Drchal, V. *Chem. Phys.* **1987**, *118*, 313.
(3) Krejčík, M.; Vlček, A. A. *J. Electroanal. Chem.* **1991**, *313*, 243.
(4) Krejčík, M.; Vlček, A. A. *Inorg. Chem.* **1992**, *31*, 2390.
(5) Sullivan, B. P.; Salmon, D. J.; Meyer, T. J. *Inorg. Chem.* **1978**, *17*, 3334.
(6) Krause, R. A. *Inorg. Chem.* **1977**, *22*, 209.

0020-1669/95/1334-6008$09.00/0

Table 1. Wave Functions and Ground State Energies for the System AB_2,[a] Described by the Hamiltonian (3) with $n = 0, 1, 2, ..., 6$ Excess Electrons

n	multiplicity	degeneracy	wave function	$E(n)$
0	1	1	$\|0\rangle$	0
1	2	1	$\|A\uparrow\rangle$	e_A
1	2	2	$\|B\uparrow\rangle$	e_B
2	1	1	$\|A\uparrow A\downarrow\rangle$	$2e_A + u_A$
2	3	2	$\|A\uparrow B\uparrow\rangle$	$e_A + e_B + v_{AB}$
2	3	1	$\|B\uparrow B\uparrow\rangle$	$2e_B + v_{BB}$
3	2	2	$\|A\uparrow A\downarrow B\uparrow\rangle$	$e_A + e_B + u_A + 2v_{AB}$
3	4	1	$\|A\uparrow B\uparrow B\uparrow\rangle$	$e_A + 2e_B + v_{BB} + 2v_{AB}$
3	2	2	$\|B\uparrow B\downarrow B\downarrow\rangle$	$3e_B + u_B + 2v_{BB}$
4	3	1	$\|A\uparrow A\downarrow B\uparrow B\uparrow\rangle$	$2e_A + 2e_B + u_A + v_{BB} + 4v_{AB}$
4	3	2	$\|A\uparrow B\uparrow B\downarrow B\uparrow\rangle$	$e_A + 3e_B + u_B + 2v_{BB} + 3v_{AB}$
4	1	1	$\|B\uparrow B\downarrow B\uparrow B\downarrow\rangle$	$4e_B + 2u_B + 4v_{BB}$
5	2	2	$\|A\uparrow A\downarrow B\uparrow B\downarrow B\uparrow\rangle$	$2e_A + 3e_B + u_A + u_B + 2v_{BB} + 6v_{AB}$
5	2	1	$\|A\uparrow B\uparrow B\downarrow B\uparrow B\downarrow\rangle$	$e_A + 4e_B + 2u_B + 4v_{BB} + 4v_{AB}$
6	1	1	$\|A\uparrow A\downarrow B\uparrow B\downarrow B\uparrow B\downarrow\rangle$	$2e_A + 4e_B + u_A + 2u_B + 4v_{BB} + 8v_{AB}$

[a] Values for systems A_2B are obtained by interchanging A for B, and vice versa, in all expressions.

U_i is the strength of the pair interaction between two electrons in the redox orbital of the same ligand $(ii|ii)$, V_{ij} is the strength of the pair interaction between two electrons on different ligands $(ii|jj)$. Hopping integrals are completely neglected in this model.

The influence of the surrounding solvent molecules can be described by a simplified Born model, using the zero differential overlap approximation,[2,11] which includes the solvent interaction in the total Hamiltonian:

$$H_{tot} = H_0 + H_s[\psi] = \sum_{i\sigma}(E_i + E^s_i + U^s_i)n_{i\sigma} + \sum_i(U_i + U^s_i)n_{i\uparrow}n_{i\downarrow} + \sum_{i\neq j}(V_{ij} + V^s_{ij})n_in_j \quad (2)$$

where the parameters E_i^s, U_i^s, and V_{ij}^s, described previously,[2] express the screening of the parameters valid for an isolated complex by the surrounding solvent. This Hamiltonian can then be written in the form:

$$H_{tot} = \sum_{i\sigma}e_in_{i\sigma} \sum_i u_in_{i\uparrow}n_{i\downarrow} + \sum_{ij}v_{ij}n_in_j \quad (3)$$

$$e_i = E_i + E^s_i + U^s_i$$

$$u_i = U_i + 2U^s_i$$

$$v_{ij} = V_{ij} + V^s_{ij}$$

The redefined parameters, e_i, u_i, and v_{ij}, include the accompanying solvation contributions. Equation 3 can be used to calculate the energies of various configurations for different number of electrons in the system.

The construction of occupation patterns and possible pathways along the redox series is quite simple for complexes of the type $MAB_2^{(2-n)+}$ or $MA_2B^{(2-n)+}$. For each number of electrons several different configurations are obtained. The energies of all possible states expressed in terms of the parameters e_i, u_i, and v_{ij} are given in Table 1. For each complex MAB_2 (or MA_2B) we have, in principle, the following possible occupation patterns shown in Chart 1 (the central atom M is omitted for simplicity, A is supposed to be always the first to undergo reduction).

Using the expressions in Table 1 it is trivial to calculate electron affinities for any of the redox steps involved, in terms of the parameters e_i, u_i, and v_{ij}. It is assumed that the entropy changes along the series are small or negligible, due to the large size of species studied.[1,12] The derivation is based on the simplification that the parameters e_i, u_i, and v_{ij} do not depend on the total number of electrons (see below). These parameters can be calculated using quantum mechanical procedures, as was done for tris-homoleptic species.[2] For the present purposes, taking into account the rather large uncertainties in the calculated values of parameters, we prefer to extract the parameters from independent experimental data.

Chart 1

	$RuAB_2$			RuA_2B	
I	II	III	IV	V	VI
ABB	ABB	ABB	AAB	AAB	AAB
$A^{\cdot}BB$	$A^{\cdot}BB$	$A^{\cdot}BB$	$A^{\cdot}AB$	$A^{\cdot}AB$	$A^{\cdot}AB$
$A^{2\cdot}BB$	$A^{\cdot}B^{\cdot}B$	$A^{\cdot}B^{\cdot}B$	$A^{\cdot}A^{\cdot}B$	$A^{\cdot}A^{\cdot}B$	$A^{\cdot}A^{\cdot}B$
$A^{2\cdot}B^{\cdot}B$	$A^{\cdot}B^{\cdot}B^{\cdot}$	$A^{\cdot}B^{\cdot}B^{\cdot}$	$A^{2\cdot}A^{\cdot}B$	$A^{\cdot}A^{\cdot}B^{\cdot}$	$A^{2\cdot}A^{\cdot}B^{\cdot}$
$A^{2\cdot}B^{\cdot}B^{\cdot}$	$A^{\cdot}B^{2\cdot}B^{\cdot}$	$A^{2\cdot}B^{\cdot}B^{\cdot}$	$A^{2\cdot}A^{2\cdot}B$	$A^{\cdot}A^{\cdot}B^{2\cdot}$	$A^{2\cdot}A^{\cdot}B^{\cdot}$
$A^{2\cdot}B^{2\cdot}B^{\cdot}$	$A^{\cdot}B^{2\cdot}B^{2\cdot}$	$A^{2\cdot}B^{\cdot}B^{\cdot}$	$A^{2\cdot}A^{2\cdot}B^{\cdot}$	$A^{2\cdot}A^{\cdot}B^{2\cdot}$	$A^{2\cdot}A^{2\cdot}B^{\cdot}$
$A^{2\cdot}B^{2\cdot}B^{2\cdot}$	$A^{2\cdot}B^{2\cdot}B^{2\cdot}$	$A^{2\cdot}B^{2\cdot}B^{2\cdot}$	$A^{2\cdot}A^{2\cdot}B^{2\cdot}$	$A^{2\cdot}A^{2\cdot}B^{2\cdot}$	$A^{2\cdot}A^{2\cdot}B^{2\cdot}$

Table 2. Proposed Patterns and Values of Parameters for Individual Complexes Where Indexes 1 and 2 Denote Mono and Bis Complexes $[RuL_m(bpy)_{3-m}]^{2+}$ of Given Ligand L and the Last Column Gives the Occupation Pattern, Confirmed Spectroelectrochemically (Except for pq and bpz)

L	$-e_L$	u_L	v_L	v_{AB}	occupation pattern
bpy	0.0	0.68	0.17		
$5dceb_1$	0.57	0.47	0.12	0.15	I
$5dceb_2$	0.57	0.47	0.12	0.15	IV
$4dceb_1$	0.38	0.40	0.15	0.16	III or I[a,b]
$4dceb_2$	0.43	0.40	0.14	0.15	IV[b]
bpm_1	0.28	0.67	0.12	0.15	III
bpm_2	0.34	0.67	0.12	0.15	VI
$bpym_1$	0.59	0.62	0.10	0.12	I[b]
$bpym_2$	0.61	0.62	0.10	0.15	IV[b]
bq_1	0.47	0.64	0.20	0.20	I or III[a]
bq_2	0.56	0.64	0.25	0.25	IV[b]
pq_1	0.23	0.60	0.14	0.15	III
pq_2	0.27	0.60	0.17	0.17	VI
bpz_1	0.42	0.63	0.15	0.15	I or III
bpz_2	0.49	0.63	0.15	0.15	IV or VI

[a] Calculation indicates best fit for I, III being very close. Spectra indicate for $n = 1$ and 2 pattern III (see Chart 1 for the individual occupation pattern and spin multiplicity). [b] For $n = 3$ or 4 the actual configuration is a mixture of two energetically close configurations

(7) (a) Wachholz, W. F.; Auerbach, R. A.; Schmehl, R. H. *Inorg. Chem.* **1986**, *25*, 227. (b) Spritschnik, G.; Spritschnik, H. W.; Kirsch, P. P.; Whitten, D. G. *J. Am. Chem. Soc.* **1977**, *99*, 4947.
(8) Effenberger, F. *Chem. Ber.* **1965**, *98*, 2260.
(9) Linderberg, J.; Ohrn, Y. *J. Chem. Phys.* **1968**, *49*, 716.
(10) Hubbard, J. *Phys. Rev. B* **1978**, 494.
(11) (a) Jano, I. *C. R. Acad. Sci. (Paris)* **1965**, *261*, 103. (b) Jano, I. *Chem. Phys. Lett.* **1984**, *106*, 60.
(12) Our measurements of redox potentials of all complexes described made at 25 and −74 °C suggest very low temperature dependence of reversible E°'s indicating thus very low entropy changes for the couples $[ML_mbpy_{3-m}]^n + Fc = [ML_mbpy_{3-m}]^{n-1} + Fc^+$; see also: Dei, A. *Inorg. Chem.* **1993**, *32*, 5730.

Table 3. Half-Wave Potentials of $[RuL_m(bpy)_{3-m}]^{2+}$ Complexes Expressed against the First Reduction Potential of $[Ru(bpy)_3]^{2+}$ as Zero (−1.80 ± 0.03 V vs Fc/Fc^+, i.e. −1.38 V vs SCE; Peak Separation 50 mV at −75 °C, DMF Containing 0.1 M TBAHF; 100 mV s^{-1})[a]

		Redox step								
L	*m*	1	2	3	4	5	6	7	8	9
5dceb	1	+0.57	+0.21	−0.26	−0.55	−1.28	−1.63			
	2	+0.64	+0.51	+0.07	−0.10	−0.64	−1.50			
	3	+0.70	+0.61	+0.45	−0.02	−0.20	−0.46			
4dceb	1	+0.38	−0.03	−0.20	−0.49	−1.08	−1.30	−1.63		
	2	+0.43	+0.28	−0.12	−0.29	−0.64	−1.19	−1.38		
	3	+0.47	+0.34	+0.18	−0.21	−0.40	−0.70	−1.19	−1.34	−1.66
bpm	1	+0.28	−0.11	−0.31	−0.77	−1.27	−1.75 (IR)			
	2	+0.34	+0.23	−0.22	−0.61	−0.97	−1.62 (IR)			
	3	+0.36	+0.26	+0.12	−0.55	−0.82	−1.28			
bpym	1	+0.59	−0.06	−0.26	−0.56	−1.29				
	2	+0.61	+0.53	−0.04	−0.26	−0.80	−1.57 (IR)			
	3	+0.64	+0.57	+0.46	−0.16	−0.45	−0.87			
bq	1	+0.47	−0.10	−0.31	−0.82	−1.40				
	2	+0.56	+0.34	−0.25	−0.56	−1.25				
	3	+0.64	+0.41	+0.05	−0.60	−0.97				

[a] IR indicates a chemically irreversible redox step.

Assuming that A is more easily reduced than B, the site energy, e_A, is identified as the first reduction potential of the given complex relative to that of B which is taken as the first reduction potential of B in the homoleptic complex MB_3^{2+}, the site energy e_B of which is set to zero. This procedure is only an approximation as e_B and e_A are to some extent interrelated, depending both on the nature and number of ligands A. However, the error which might be created by this approach is relatively small, as can be seen from the slopes of plots of $E^0_1 - m$ (E^0_1 = first reduction potential; m = number of ligands A in the complex) which is about 50 mV for A and B not strongly different in their electron-withdrawing abilities.[13] (Further refinement can be obtained by successive approximations.) Values u_A, u_B, v_{AA}, and v_{BB} are estimated from the differences in reduction potentials of corresponding homoleptic complexes, MA_3^{2+} and MB_3^{2+}, respectively, using the equations derived previously for this type of complex.[2] v_{AB} is usually approximated as an average of v_{AA} and v_{BB}.

Using expressions given in Table 1 and parameters from Table 2, energies of various electronic configurations are calculated for each number of excess electrons (n) in the system. From these data the sequence of redox potentials can easily be calculated for each occupation scheme given above. Calculated redox potentials correspond to one-electron changes. If the redox potential, E^0_{n+1}, appears to be more positive than the preceding one, E^0_n, a two electron wave results, as the product of the nth process must be immediately reduced to the (n + 1)th product. By this procedure the pattern of the redox series is obtained in terms of redox potentials and corresponding numbers of electrons. By comparison of the estimated pattern with the experimental one the most probable occupation pattern is easily established.

Thermodynamics requires that the reduction path taken by any system is always that following the most stable configurations, i.e. those with the most negative energies. This strict requirement might in special cases result in crossing from one occupation pattern to another. If the energies for all configurations in pattern X are lower than those in pattern Y, except for one step which is more stable in pattern Y, then this configuration is to be included into the occupation pattern. Inspection of the basic occupation patterns reveals that this might occur when addition of the (n + 1)th electron causes a decoupling of spins already paired in one of the previous steps.

In some systems, a very special feature may appear: for some sets of parameters, especially for particular combinations of site and spin-pairing energies, two different configurations for the same n have identical, or very close, energies. This means that both configurations would be formed with the same, or very similar, probability. The product is either a mixture of species that belong to different configurations with respective weights, or a complex in the quantum-mechanical state ψ_R described as a linear combination of two energetically identical or very close lying configurations, e.g. $\psi_R = a\psi(A^2{}^-B^-B) + b\psi(A^-B^-B^-)$ (a, b = mixing coefficients). Both these above mentioned states influence optical spectra in a similar way. This conclusion,brings new insight on the formulation of reduction product in general.

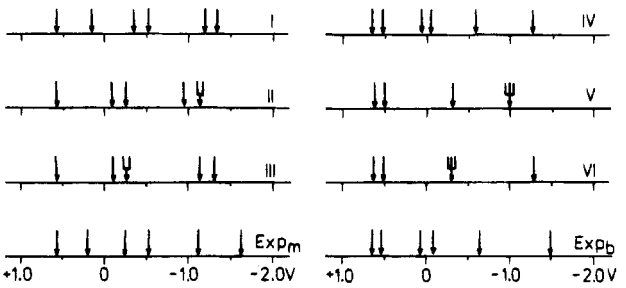

Figure 1. Comparison of experimental and calculated redox potentials for the redox series of complexes $[Ru(5dceb)(bpy)_2]^{(2-n)+}$ and $[Ru(5dceb)_2(bpy)]^{(2-n)+}$; Capital Roman letter indicates the occupation pattern. Exp_m and I, II, and III are for monosubstituted and Exp_b and IV, V, and VI are for bis complexes (Exp = experimental values). The first reduction of tris(bipyridine)ruthenium(II) is taken as zero. Key: double arrow, two electron wave; triple arrow, three electron wave.

Results and Discussion

Even though the electrochemical behavior of most of the complexes described below has already been reported, we have, in most cases, remeasured them under identical conditions. All complexes were investigated at −74 °C, the most suitable temperature. All reduction steps were electrochemically and chemically reversible, unless otherwise noted (see Table 3).

The analysis was carried out for the redox series of two types of complexes: mono-L, $[RuLbpy_2]^{2+}$, and bis-L, $[RuL_2bpy]^{2+}$, with L = bq, 4decb, 5decb, bpm, bpym, 2-(2-pyridyl)quinoline (pq), and 2,2′-bipyrazine (bpz); the data for the last two sets were taken from refs 14−16 (L ≡ A, bpy ≡ B). For each complex, data were calculated for relevant occupation patterns only, i.e. for those starting with the reduction of the more easily reducible ligand.

The procedure is illustrated in Figure 1 for redox series $[Ru(5decb)(bpy)_2]^{(2-n)+}$ and $[Ru(5decb)_2(bpy)]^{(2-n)}$. This figure

(13) Vlček, A. A.; Lever, A. B. P. Unpublished results.

(14) Elliott, C. M.; Hershenhart, E. J. *J. Am. Chem. Soc.* **1982**, *104*, 7519.
(15) Ohsawa, Y.; Hanck, K. W.; DeArmond, M. K. *J. Electroanal. Chem.* **1984**, *175*, 229.
(16) Juris, A.; Campagna, S.; Balzani, V.; Gremaund, G.; von Zelewsky, A. *Inorg. Chem.* **1988**, *27*, 3652.

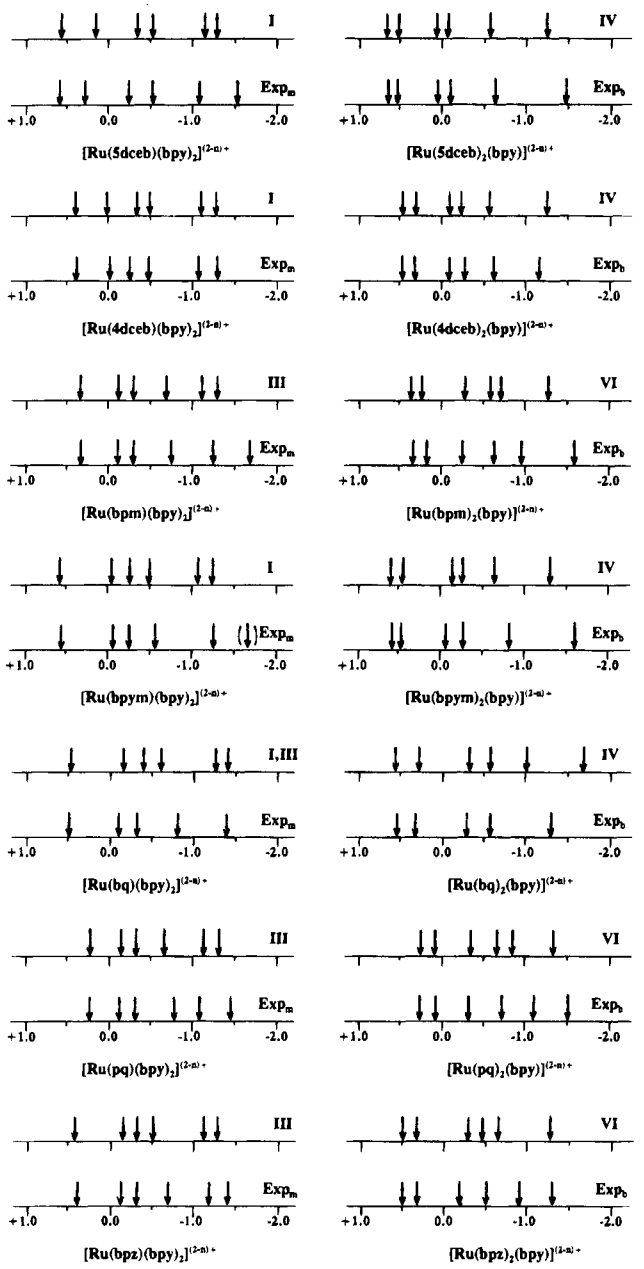

Figure 2. Comparison of experimental redox potentials for the redox series of complexes $[RuLbpy_2]^{2+}$ and $[RuL_2bpy]^{2+}$ and calculated ones for the most probable occupation pattern. L is as follows: 5decb, 4dceb, bpm, bpym, bq, pq, bpz. Exp_m and Exp_b are experimental values for mono- and bis-substituted complexes, respectively. A capital roman letter indicates the most probable occupation pattern. The first reduction of tris(bipyridine)ruthenium (II) is taken as zero.

shows that experimental redox potential sequences are well reproduced by calculations for occupation patterns I and IV only. Quantitative agreement between experimental and calculated sets is usually observed for the first three or four reduction steps only. The most negative waves observed experimentally agree only qualitatively with the calculated ones (see below).

The experimental redox potentials together with calculated sequences for the most probable patterns are collected and presented in Figure 2.[17]

Two basically different types of behavior are observed.

Species with $(e_A - e_B) > u_A$, i.e. ***with relative site energy larger than the spin pairing energy***, follow pattern I for mono-L or IV for bis-L species, respectively. This behavior corresponds to full spin-pairing of electrons in the L-species prior to reduction of bpy.

(17) Note that the parameters are determined for −74 °C. At other temperatures different parameters would, of course, result and the computed pattern of redox potentials would be slightly different. All spectra, on the other hand, were measured at 20 °C.

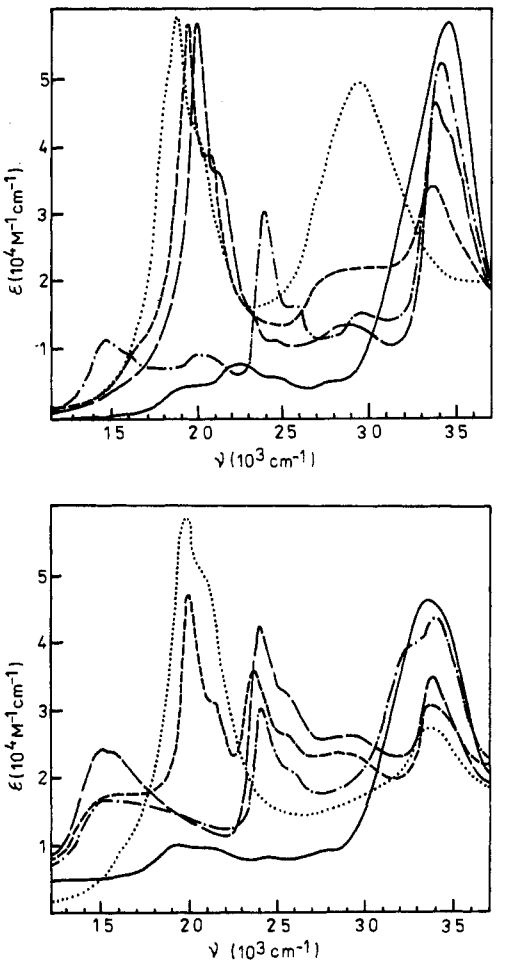

Figure 3. Electronic absorption spectrum of $[Ru(5dceb)(bpy)_2]^{(2-n)+}$ (top) and $[Ru(5dceb)_2(bpy)]^{(2-n)+}$ (bottom). Key: (—) $n = 0$; (—·—) $n = 1$; (— —) $n = 2$; (- -) $n = 3$; (···) $n = 4$. Spectroelectrochemical measurements were performed in 0.1 M TBAH/DMF solution.

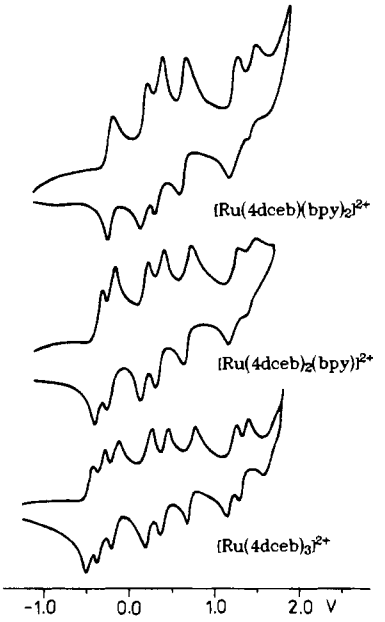

Figure 4. Cyclic voltammograms of $[Ru(4dceb)_n(bpy)_{3-n}]^{2+}$ complexes expressed against the first reduction potential of $[Ru(bpy)_3]^{2+}$ as zero (−1.80 ± 0.03 V vs Fc/Fc^+, i.e. −1.38 V vs SCE; peak separation 50 mV at −75 °C, DMF containing 0.1 M TBAH; 100 mV s^{-1}).

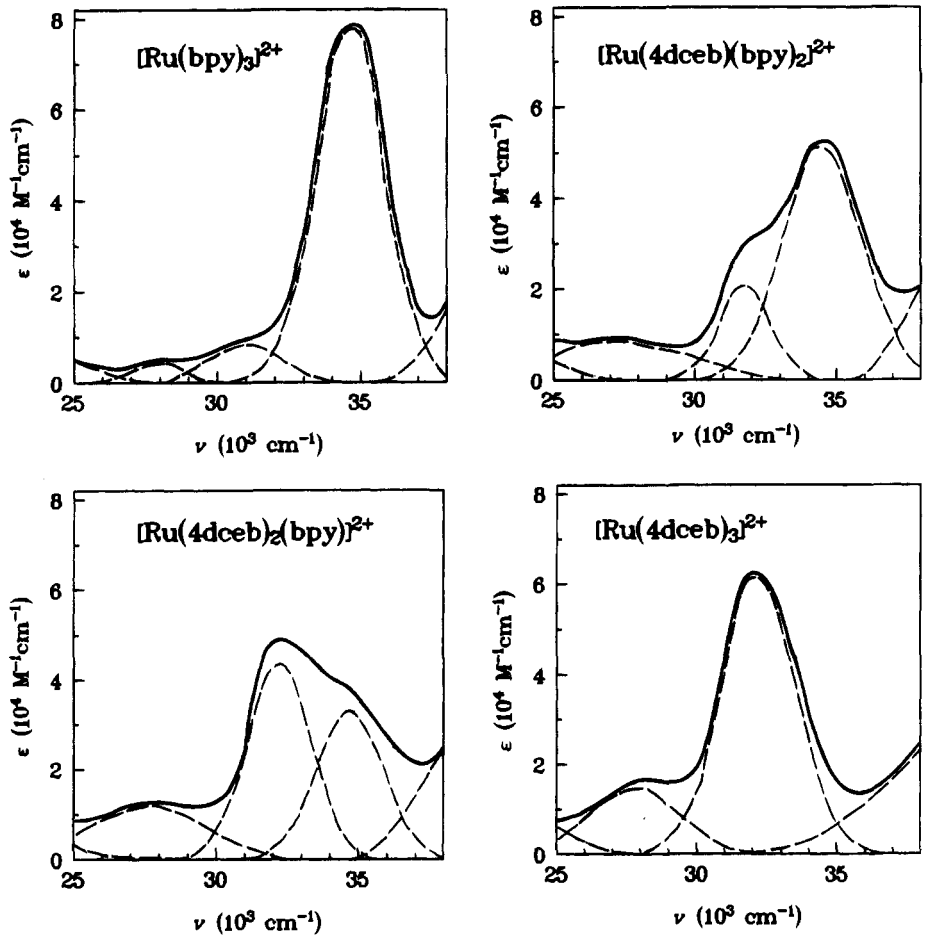

Figure 5. Deconvoluted electronic absorption spectra of $[Ru(4dceb)_m(bpy)_{(3-m)}]^{2+}$ complexes (m = 0, 1, 2, 3). Key: (−) experimental spectrum; (− −) deconvoluted Gaussian features.

Species with $(e_A - e_B) < u_A$, i.e. ***with relative site energy lower than the spin pairing energy***, follow pattern III for mono-L or VI for bis-L species, respectively. This behavior corresponds to one electron stepwise reduction of all ligands always keeping the spin of the system at maximum possible value.

Systems in which the relative site energy is close to the spin pairing energy are to be analyzed very carefully. Small uncertainties in the parameters might cause wrong conclusions. In these cases the spectroelectrochemical confirmation of the predicted pattern is essential.

In Table 2 the occupation patterns for $ML(bpy)_2$ and $ML_2(bpy)$ are given. Redox series for which a unique configuration cannot be specified (n = 2 or 3) are noted. For bpz complexes, the combination of parameters does not make it possible to distinguish qualitatively between patterns I and III or IV and VI, for the mono- and bis-L species, respectively. It might be mentioned that this result can be extended for tris heteroleptic complexes. For example in $[Ru(bq)(bpy)L]^{2+}$ series even configurations such as $[Ru(bq^-)(bpy)L^{2-}]^-$ may play an important role.

Spectroelectrochemistry can be used to confirm the occupation configurations in those systems in which it is possible to identify the absorption features of components of coordination sphere.[8,18,19] The redox series of 4,4′- and 5,5′- dicarboxyethyl complexes can serve as an illustrative example. A straightforward proof of occupation patterns I and IV, respectively, is given by analysis of spectra of redox series $[Ru(5decb)(bpy)_2]^{(2-n)+}$ and $[Ru(5decb)_2(bpy)]^{(2-n)+}$ in which the various redox forms of coordinated ligands can be clearly identified (approximate υ_{max}:[19,20] bpy = 34 000 cm^{-1}, bpy^- = 30 000 cm^{-1}, 5dceb = 32 000 cm^{-1}, $5dceb^-$ = 26 000−26 500 cm^{-1}, and $5dceb^{2-}$ = 21 000−22 000 cm^{-1}) (see Figure 3).

Electronic spectra of first reduction product of $[Ru(4decb)(bpy)_2]^{(2-n)+}$ and $[Ru(4decb)_2(bpy)]^{(2-n)+}$ series whose cyclic voltammograms are depicted in Figure 4 can be analyzed in a similar manner. The deconvoluted spectra (using symmetrical Gaussians) of nonreduced species (Figure 5) indicate the additive properties of ligand based features which is valid also for other complexes examined. Figure 6 shows the good agreement of experimental spectra with simulated spectra. Simulated spectra were obtained by weighted averaging of corresponding spectra of tris homoleptic complexes $[Ru(bpy)_3]^{2+}$,$[Ru(bpy)_3]^-$, $[Ru(4decb)_3]^{2+}$, $[Ru(4decb)_3]^-$, and $[Ru(4decb)_3]^{2-}$ in the region of internal ligand transitions. In simulated spectra of mixed-ligand complexes, each oxidation state of homoleptic complex contributes by one-third of its intensity multiplied by stoichiometric coefficient to the whole spectrum. The simulation of spectra can be carried out only in the region of intraligand transitions, no MLCT can be simulated. Simulation is carried out under the assumption that the spectral features of intraligand transitions obtained from corresponding tris homoleptic species of appropriate charge do not change in

(18) E.g.: (a) Donohoe, R. J.; Tait, C. D.; DeArmond, M. K.; Wertz, D. W. *J. Phys. Chem.* **1986**, *90*, 3923. (b) Donohoe, R. J.; Tait, C. D.; DeArmond, M. K.; Wertz, D. W. *J. Phys. Chem.* **1986**, *90*, 3927. (c) Fees, J.; Kaim, W.; Moscherosch, M.; Matheis, W.; Klíma, J.; Krejčík, M.; Záliš, S. *Inorg. Chem.* **1993**, *32*, 166.

(19) Gaš, B.; Klíma, J.; Záliš, S.; Vlček, A. A. *J. Electroanal. Chem.* **1987**, *222*, 161.

(20) Gaš, B.; Vlček, A. A. Unpublished results.

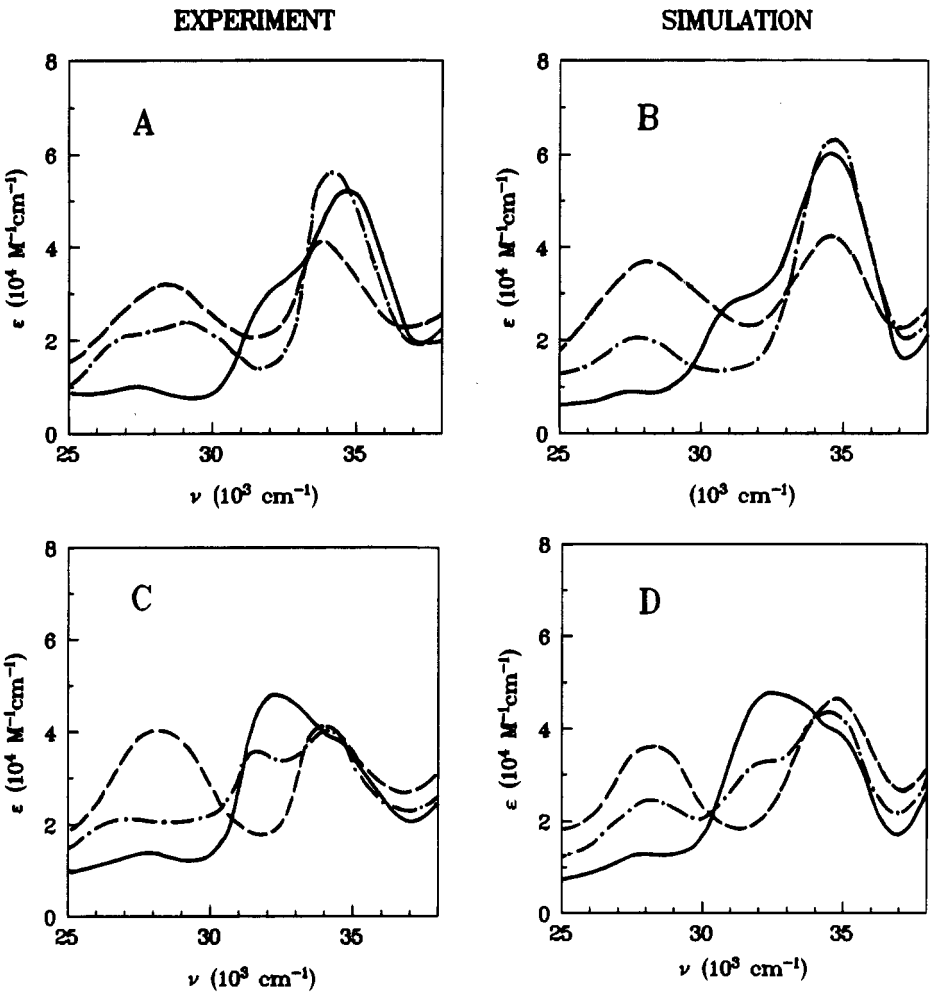

Figure 6. Experimental and simulated electronic absorption spectra of $[Ru(4dceb)(bpy)_2]^{(2-n)+}$ (A - experimental, B - simulated) and $[Ru(4dceb)_2(bpy)]^{(2-n)+}$ (C - experimental, D - simulated). (—) $n = 0$; (—·—) $n = 1$; (···) $n = 2$.

heteroleptic species by more then about 10%. The validity of this procedure is clearly demonstrated by spectra of $[Ru(5decb)_n(bpy)_{3-n}]^{(2-n)+}$ species given in Figure 3 in which only a slight shift of ν_{max} is observed with increasing overall charge.

A more complicated situation arises for lower oxidation states of 4dceb complexes. The inspection of the calculated energies of products for $n = 2$ and 3 of the mono species and for $n = 3$ and 4 of the bis species, respectively, reveals that energies of some products are quite close:

$[Ru(4dceb^{2-})(bpy)_2]$	-0.36 eV
$[Ru(4dceb^{-})(bpy^{-})(bpy)]$	-0.23 eV
$[Ru(4dceb^{2-})(bpy^{-})(bpy)]^{-}$	+0.08 eV
$[Ru(4dceb^{-})(bpy^{-})(bpy^{-})]^{-}$	-0.06 eV
$[Ru(4dceb^{2-})(4dceb^{-})(bpy)]^{-}$	-0.61 eV
$[Ru(4dceb^{-})(4dceb^{-})(bpy^{-})]^{-}$	-0.43 eV
$[Ru(4dceb^{2-})(4dceb^{2-})(bpy)]^{2-}$	-0.36 eV
$[Ru(4dceb^{2-})(4dceb^{-})(bpy^{-})]^{2-}$	-0.17 eV

The energies of the above configurations formed by bis-4dceb complexes become almost identical when the interligand electronic repulsion becomes slightly less (from $v_{AB} = 0.15$ to $v_{AB} = 0.10$ eV). Thus the reduction paths of the 4dceb complexes follow predominantly occupation patterns I and IV, with mixed configurations for $n = 2$ and 3 and $n = 3$ and 4 for mono- and bis-4dceb complexes, respectively. This situation is reflected in the spectra of the reduction products. As can be seen from Figure 7, the spectra of $[Ru(4decb)_2(bpy)]^-$ cannot be fitted either by assuming configuration

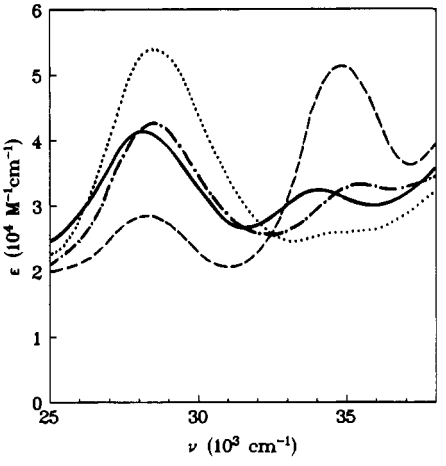

Figure 7. Experimental and simulated electronic absorption spectra of $[Ru(4dceb)_2(bpy)]^-$. Key: (—) experiment; (– –) $[Ru(4decb^{2-})(4decb^{-})bpy]^-$; (···) $[Ru(4decb^{-})_2bpy^-]^-$; (—·—) mixing of calculated spectra of configurations $[Ru(4decb^{2-})(4decb^{-})bpy]^-$ and $[Ru(4decb^{-})_2bpy^-]$ with weights 0.65 and 0.35, respectively.

$[Ru(4decb^{2-})(4decb^{-})(bpy)]^-$or by configuration $[Ru(4decb^{-})_2(bpy^{-})^-$ only. The best fit between simulated and experimental spectra is obtained by mixing the calculated spectra of configurations $|A^-A^-B^-\rangle$ and $|A^{2-}A^-B\rangle$ with weights 0.65 and 0.35, respectively.

Experimental data show always larger separations of experimental E^0 values in the more negative region, compared to the calculated data. This fact has been noted previously and

discussed [1,2] for tris homoleptic RuL_3^{2+} species. It seems to be due to the change in parameters describing the energy of the system with the overall number of electrons on individual ligands. As the number of electrons in the system increases, the electron−electron interactions increase. This effect can be seen in the reduction of $Rubpy_3^{2+}$ for which the occupation pattern is unambiguous. The difference between the first and second reduction potentials is 0.17 V, which corresponds very closely to the interligand electron−electron interaction in electron-poor systems. The difference between the fifth and sixth reduction potentials is about 0.30 V, which corresponds to an analogous interaction, but in more electron rich systems in which stronger electron−electron repulsion is expected.

The method can also be applied to elucidate some apparently unexpected behavior. For example the reduction pattern of $[(A_2Ru-BiBzIm-RuB_2]$ (A = 5dceb, BiBzIm = 2,2′-dibenzoimidazolate dianion, B = bpy) indicates the following number of electrons in individual steps: 1 1 1 2 1 1.[21] The calculated pattern gives the same set of electron numbers. The two electron wave results from the overlap of the process of accepting the fourth electron, completing the reduction of the RuA_2 unit, with that of accepting the fifth electron, corresponding to the first reduction of the RuB_2 unit. The calculation indicates that the latter process occurs about 50 mV more positive than the former one. The later reduction steps follow the normal $Ru(bpy)_2$ redox series.

Acknowledgment. The authors are indebted to the Granting Agency of the Czech Republic (S.Z. for Grant No. 203/94/1492, V.D. for Grant No. 11037).

IC941245D

(21) Haga, M.; Bond, A. M. *Inorg. Chem.* **1991**, *30*, 478.